The dermal arteries in the cutaneous angiosome of the descending genicular artery

Ines E. Tinhofer,[1] iD Maximilian Zaussinger,[1] Stefan H. Geyer,[1] iD Stefan Meng,[1,2] Lars-Peter Kamolz,[3,4] Chieh-Han J. Tzou[5] and Wolfgang J. Weninger[1]

[1]Division of Anatomy, Centre for Anatomy and Cell Biology, Medical University of Vienna, Vienna, Austria
[2]Department of Radiology, Kaiser-Franz-Josef Hospital, Vienna, Austria
[3]Division of Plastic, Aesthetic and Reconstructive Surgery, Department of Surgery, Medizinische Universitat Graz, Graz, Austria
[4]COREMED - Cooperative Centre for Regenerative Medicine, Joanneum Research GmbH, Graz, Austria
[5]Plastic and Reconstructive Surgery, Department of Surgery, Hospital of the Divine Saviour, Vienna, Austria

Abstract

Studies examining thick skin of the thumb pad have challenged the existence of an arterial plexus in the papillary dermis. Instead of a plexus, discrete arterial units, interconnected by arterio-arterial anastomoses, were identified. We hypothesise that the dermal arteries of thin skin are arranged likewise and that there are fewer arterio-arterial anastomoses in the centre of an angiosome than in zones where neighbouring angiosomes overlap. To test these hypotheses, we examined the dermal arteries in the centre of the cutaneous angiosome of the descending genicular artery (DGA) and its zone of overlap with neighbouring angiosomes. Using traditional perfusion techniques, the cutaneous angiosomes of the DGA and the popliteal artery were identified in 11 fresh frozen human lower limbs. Biopsies were harvested from the centre of the cutaneous DGA angiosome and from the zone where neighbouring vascular territories overlapped. Employing high-resolution episcopic microscopy (HREM), digital volume data were generated and the dermal arteries were three-dimensionally reconstructed and examined. In all examined skin areas, the dermal arteries showed tree-like ramifications. The branches of the dermal arteries were connected on average by 1.73 ± 1.01 arterio-arterial anastomoses in the centre of the DGA angiosome and by 3.27 ± 1.27 in the zone where angiosomes overlapped. We demonstrate that discrete but overlapping dermal arterial units with a mean dimension of 1.62 ± 1.34 and 1.80 ± 1.56 mm^2, respectively, supply oxygen and nutrients to the superficial dermis and epidermis of the thin skin of the medial femur. This forms the basis for diagnosing and researching skin pathologies.

Key words: anatomy; blood vessel architecture; cutis; high resolution episcopic microscopy; skin.

Introduction

Blood supply to the cutaneous and skeletomuscular system is organized in macroscopic units, called angiosomes. This term was first introduced by Taylor in 1987 and defines a three-dimensional tissue volume that is exclusively supplied by branches of a singular source artery (Taylor & Palmer, 1987). The cutaneous parts of an angiosome can be defined as volumes of skin and subcutaneous tissue supplied by branches of an artery that perforates the body fascia. Such cutaneous units, which are supplied by a perforator artery, are also referred to as perforasomes.

Adjacent angiosomes and perforasomes are connected by arterio-arterial anastomoses and various arterial plexi. Usually these connections are sufficient for securing blood flow in a skin volume supplied by a defective perforator artery by hyperperfusion of neighbouring perforasomes (Saint-Cyr et al. 2009).

According to anatomical and dermatological textbooks, blood exchange between neighbouring angiosomes is guaranteed by two horizontally orientated arterial plexi. One is located at the dermo/hypodermal junction (profound plexus) and the second in the papillary stratum of the dermis (superficial plexus; Spalteholz, 1927; Horstmann, 1957; Manchot, 1983). Parallel with the dermal arterial plexus, venous plexi are formed. All these dermal plexi play an important role in thermoregulation and the arterial plexi are considered to guarantee a smooth supply of oxygen

and nutrients to the epidermal and dermal skin layers even in the case of focal vascular diseases or injuries, which affect single vessels feeding the plexi (Taylor & Minabe, 1992).

In addition to the two dermal plexi, a third arterial and a venous plexi exist in many skin areas. These plexi comprise large interconnecting branches of subcutaneous blood vessels, which are located in the deep strata of the the subcutis (subcutaneous plexi).

The angiosome concept and the peculiar arrangement of the subcutaneous and dermal blood vessels have attracted the attention of plastic surgeons since the late 1980s because precise knowledge of blood supply to the skin is of special importance for designing skin flaps (Kroll & Rosenfield, 1988; Koshima & Soeda, 1989). Furthermore, such knowledge is essential for understanding the genesis of skin pathologies as well as for developing new concepts for their treatment.

Hence, various sophisticated but essentially simple imaging methods for analysing the extension of angiosomes were developed in the last decades and immediately successfully applied for researching vascular skin territories (Braverman et al. 1990; Ikeda et al. 1991; Hasegawa et al. 2001; Zhang et al. 2011; Dalimier & Salomon, 2012). Visualising the complex architecture of dermal blood vessels has been more challenging. Recently, a three-dimensional (3D) imaging method, high resolution episcopic microscopy (HREM), was developed for visualising embryo morphology (Weninger et al. 2006; Geyer et al. 2009; Mohun & Weninger, 2012b). In the last few years this method has also been applied for analysing the topology of dermal arteries in humans and biomedical models (Weninger et al. 2006; Mohun & Weninger, 2012b; Geyer et al. 2013, 2014, 2015; Wiedner et al. 2014; Wong et al. 2016). As a first result, HREM analysis of the thick skin of the human thumb pad challenged the postulate of a superficial dermal arterial plexus. Careful analysis of HREM data revealed that the dermal arteries of the thumb pad form tree-like ramifications and feed blood to circumscript dermal volumes (arterial units) instead of draining into a papillary arterial plexus (Geyer et al. 2013). We hypothesise that a similar vascular arrangement can also be detected in thin skin.

Therefore, the first aim of this study was to test this hypothesis by exemplarily analysing the arrangement of the dermal arteries of the thin skin of the medial and distal femur, in particular of the cutaneous angiosome of the descending genicular artery (DGA), which is the primary source of its blood supply.

A defective perforator artery can be functionally replaced by blood transfer from adjacent angiosomes (Saint-Cyr et al. 2009). This effect is explained by the existence of both arterio-arterial anastomoses and the various skin plexi. Our concept of dermal arterial units will challenge the existence of a superficial dermal plexus as a source of blood exchange at the level of the terminal segments of vascular territories. We therefore expect that instead of a plexus, a larger number of arterio-arterial anastomoses exist in the zone in which vascular territories overlap in order to ensure smooth blood exchange between neighbouring cutaneous angiosomes. The second aim of our study is therefore to test this hypothesis, which builds on of the first goal of our study.

Methods

This study was conducted at the Division of Anatomy of the Medical University of Vienna after ethical approval was obtained (EK number 2128/2015). Eleven lower extremities of 10 fresh human body donors (three females, seven males) were examined. Mean age of the body donors was 81.47 ± 7.90 years (range 69.40–92.43).

The vascular skin territories of the distal medial femur were demarcated using a recently established perfusion technique. The femoral artery and its branches were exposed inside the adductor canal. A 12-gauge hose connector (Connector straight, conical spout 3–5 mm, Koehler GmbH) was inserted into the femoral artery immediately proximal to the origin of the DGA and the femoral artery was ligated distal to its origin in order to perfuse the angiosome of the DGA. In addition, the popliteal artery was exposed and a 12-gauge hose connector was inserted. The artery was ligated proximal and distal to the popliteal fossa and the branches of the popliteal artery were perfused. Both hose connectors were connected to arthroscopy pumps (Arthroscopy pump AR6400 Continuous Wave™ II, Arthrex) via 4×6 mm latex hoses (Ruesch Latex-Tube 15 m, 4×6 mm, Teleflex Medical GmbH). A 0.1% aliquot of methylene blue solution [Methylenblue (C.I. 52015) reinst., Fa. LabChem, Röttinger, Germany] was pumped into the DGA with a pressure of 100 mmHg and a flow of 20 mL min^{-1}. Simultaneously, Ringer solution stained with 1.0 g eosin per 100 mL [Eosin spritlöslich (C.I. 45386) Waldeck GmbH & Co. KG, Munster, Germany] was pumped into the popliteal artery with the same settings. This procedure defined the cutaneous angiosomes of the DGA and its surrounding angiosomes, simulating physiologic conditions as closely as possible.

Two 4-mm biopsies were harvested from each specimen using biopsy punches (Biopsy Punch, Stiefel®). One biopsy was taken from the centre of the angiosome of the DGA and the other from the zone where it overlapped with the angiosomes of the branches of the popliteal artery. The biopsy material was fixed for at least 5 days in a solution comprising 4% carbolic acid and 2% neutral buffered formaldehyde and then stored in a fresh solution until further processing, according to our protocols for preparing fresh biopsy material (Geyer et al. 2014).

From all biopsy cylinders, digital volume data were created using the HREM technique (Weninger et al. 2006; Mohun & Weninger, 2010; Geyer et al. 2017). The material was removed from the storing solution and rinsed under running tap water for 12 h. Then it was dehydrated in a series of ethanols (50%, 70%, 80%, 90%, 96%). Each ethanol contained 0.4 g eosin per 100 mL. Samples were kept for 2–3 h in each solution. Dehydration was followed by infiltration of specimens in solution A of the JB-4 Plus® embedding kit containing 0.4 g eosin and 1.25 g benzoyl peroxide (plasticised catalyst) per 100 mL. Finally, the specimens were embedded in a mixture of 100 mL Solution A, 1.25 g benzoyl peroxide (plasticised catalyst) and 4 mL Solution B of the JB4 kit, to which 0.4 g eosin per 100 mL was added (Geyer et al. 2009; Mohun & Weninger, 2012a). The blocks were sealed airtight for 48 h and then stored at room temperature until digital data generation was started.

HREM volume data generation was performed according to established protocols using our prototype of an HREM apparatus

(Weninger et al. 2006; Mohun & Weninger, 2012b,c; Geyer et al. 2017). Each volume dataset comprised 2000–2300 inherently aligned digital images. As two different cameras were used for image capturing, the HREM data had a voxel size of $0.74 \times 0.74 \times 1.5 \, \mu m^3$ (12 biopsies) and $1.48 \times 1.48 \times 1.5 \, \mu m^3$ (10 biopsies), respectively.

The raw HREM data were transferred to personal computers (PCs) with high-end graphic cards (Nvidia GeForce GTX 580) and 128 GB RAM and processed using AMIRA software 5.4.5® (FEI Visualization Sciences Group). Large subcutaneous arteries were identified using traditional histological criteria. Their branches, sub-branches and anastomoses were traced through the whole volume of data and manually outlined to create binary data of the arteries. Except for the terminal capillary slings, no other capillaries were traced or analysed. Whenever possible, interpolation techniques described in recent publications were employed (Geyer et al. 2013). The binary data were then used for creating 3D surface models which, together with virtual reslices, were used for analysing the topology and interconnections of the dermal arteries.

In addition, the area of the epidermis, which was reached by the branches of a single dermal arterial unit, was defined by the branches of the respective artery and measured using IMAGEJ® software (ImageJ, Version 1.45, National Institutes of Health, USA). This was done only for those arterial units which had all their ramifications and branches within the field of view.

The field of view used for HREM data generation was rectangular and was larger in its corners than were the roundish biopsy cylinders. Consequently, some parts of the corners of the digital volume data did not contain biopsy material and the total size of the volume in the field of view varied between individual biopsies. For the sake of clarity and comparability of blood vessel numbers, we therefore selected a central section of 2.4×2.4 mm of the HREM images of each biopsy in which we counted and measured the vessels.

Statistical analyses were performed in EXCEL (Microsoft® Excel, Version 15.4) and SPSS (IBM Corp. SPSS Statistics, Version 22.0) using mean value and standard deviation calculations, as well as the t-test to confirm significant results.

Results

The average epidermal surface displayed in the images of the biopsies measured $6.65 \pm 1.34 \, mm^2$. For the sake of comparability, the number of arteries and arterio-arterial anastomoses was counted and calculated for a selected volume of data with a base area of $5.76 \, mm^2$.

Architecture of dermal arteries

In all biopsies, the arteries of the dermis, dermo-hypodermal junction and adjacent parts of the hypodermis showed a similar principal arrangement (Fig. 1). However, there were differences in the architecture and number of arteries identified in the centre of the cutaneous angiosome of the DGA and its overlapping zone with neighbouring angiosomes (Table 1).

Centre of cutaneous angiosomes of the DGA

Horizontally arranged arteries with a mean diameter of $89.67 \pm 27.65 \, \mu m$ (range 55.41–153.30 μm) crossed the

biopsy volumes at the dermo/hypodermal junction. They gave rise to 1.45 ± 1.04 (range 0–3) arteries, which ascended and ramified in the dermis. In addition to these arteries, 2.82 ± 1.72 (range 1–6) dermal arteries entered the defined data volume at the level of the dermo/hypodermal junction or profound dermis from a lateral direction (Fig. 1A,D). Due to their arrangement, size and observations in data displaying a larger volume of data than used for analysis, we feel save in considering these arteries dermal arteries arising from the horizontally orientated arteries outside of the reconstructed and analysed data volume (Fig. 1D). Hence, in total the volume of data contained stems of 4.27 ± 1.35 dermal arteries (range 3–7) with a mean diameter of $46.68 \pm 12.57 \, \mu m$ (Table 1). The stems of the dermal arteries ascended towards the superficial dermis taking a straight or arched course. While ascending, they ramified in a tree-like fashion and formed 8–14 (mean 11.36 ± 1.86) generations of branches. The terminal branches had a mean diameter of $7.40 \pm 0.68 \, \mu m$ and continued as ascending segments of capillary slings (Table 1).

None of the specimens showed a superficial arterial plexus. Instead, we identified 0–4 (1.73 ± 1.01) anastomoses connecting branches of the 2nd to 13th generation of neighbouring dermal arteries (Table 1, Fig. 2A). The anastomoses were located $654.10 \pm 233.40 \, \mu m$ below the border of stratum corneum to stratum granulosum of the epidermis. Their lumen diameters were $25.71 \pm 6.22 \, \mu m$. All 21 anastomoses connected branches of neighbouring dermal arteries or branches of arteries entering the dataset laterally. No anastomoses connected branches arising from the same dermal artery. The terminal branches of the tree-like ramifying dermal arteries reached the most superficial parts of the dermis in an area of $1.62 \pm 1.34 \, mm^2$. Branches of neighbouring dermal arteries overlapped in a mean total area of $0.90 \pm 0.91 \, mm^2$ (Fig. 2B).

Zone where neighbouring cutaneous angiosomes overlap

In the zone where the angiosome of the DGA overlaps with neighbouring angiosomes, the dermo/hypodermal junction held horizontally arranged arteries with a diameter of $94.33 \pm 32.18 \, \mu m$ (range 57.97–189.17). These arteries gave rise to 1.45 ± 0.93 (range 0–3) arteries, which entered the profound dermis within the examined volume of data. In addition, 2.18 ± 1.47 (range 0–4) dermal arteries entered the dermo-hypodermal junction or profound dermis from a lateral direction. Hence a total of 3.64 ± 1.57 (range 1–6) dermal arteries, with a diameter of $45.23 \pm 11.60 \, \mu m$ ascended from the profound dermis. These arteries ramified in a tree-like fashion and formed 7–15 (mean 12.45 ± 2.30) generations of branches (Table 1; Fig. 2C). No specimen showed an arterial plexus in the papillary dermis.

One to five (mean 3.27 ± 1.27) arterio-arterial anastomoses with a diameter of $25.19 \pm 9.50 \, \mu m$ connected the
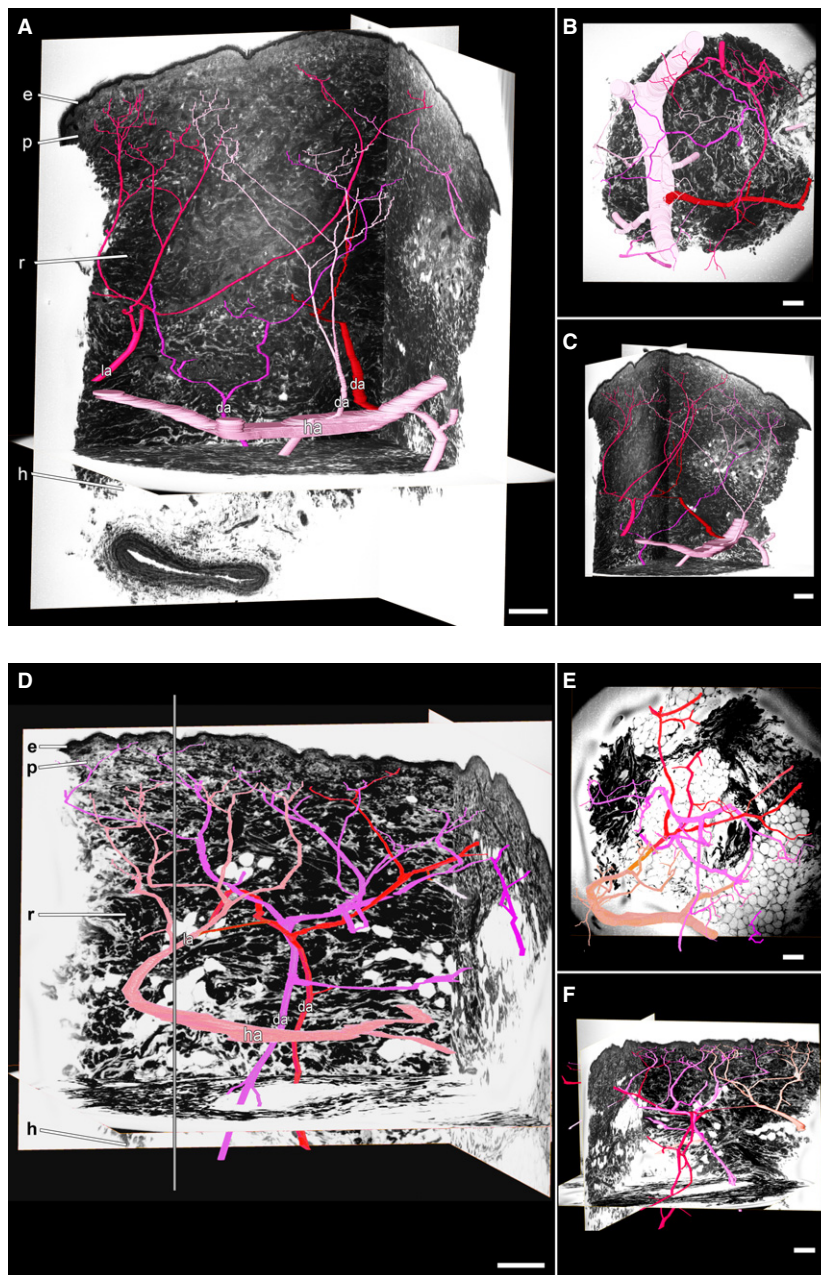
Fig. 1 Arteries in thin skin of the DGA angiosome. 3D surface models of the arteries in light pink, dark pink, red and purple in front of virtual HREM sections. The different colours are supposed to facilitate distinction of the arteries and 3D analysis. (A–C) Arrangement of the hypodermal (ha) and dermal (da) arteries with branches in the zone in which the DGA angiosome and neighbouring angiosomes overlap. View from (A) lateral, (B) superficial and (C) again lateral, but switched 90° in respect to A. (D–F) Arrangement of the dermal arteries in the centre of the DGA angiosome. Viewing point in (D) and (E) is similar to that in (A) and (B). Viewing point in (F) is rotated 180° in respect to (D). Note the dermal arteries, which enter the examined volume (defined by a grey border line in D) from lateral (la). e, epidermis; h, hypodermis; p, papillary dermis; r, reticular dermis. Scale bars: 250 μm.

1st to 14th generation of branches of the dermal arteries. This number was significantly ($P = 0.00496$) larger than the number of anastomoses detected in the centre of the angiosome (Table 1). The arterio-arterial anastomoses were a mean distance of 603.48 ± 276.21 μm beneath the transition of stratum granulosum to stratum corneum. Nine

(14.29%) anastomoses connected branches arising from the same dermal artery and 54 (85.71%) anastomoses connected branches of neighbouring dermal arteries or arteries entering the volume of data laterally.

The terminal branches of the tree-like ramifying dermal arteries reached the most superficial parts of the dermis in

Table 1 Comparison of numbers and dimensions of dermal arteries and their anastomoses in the centrum of the cutaneous DGA angiosome and its zone of overlap with neighbouring angiosomes.

	Centre of angiosome (mean ± SD)	Zone of overlap (mean ± SD)
HA		
Number	2.27 ± 1.27	1.73 ± 0.65
	range: 1–5	range: 1–3
Ø [µm]	89.67 ± 27.65	94.33 ± 32.18
	range: 55.41–153.3	range: 57.97–189.17
DA		
Number	1.45 ± 1.04	1.45 ± 0.93
	range: 0–3	range: 0–3
LA		
Number	2.82 ± 1.72	2.18 ± 1.47
	range: 1–6	range: 0–4
DA+LA		
Number	4.27 ± 1.35	3.64 ± 1.57
	range: 3–7	range: 1–6
Ø [µm]	46.68 ± 12.57	45.23 ± 11.60
	range: 29.34–89.53	range: 27.18–81.78
Generations	11.36 ± 1.86	12.45 ± 2.30
	range: 8–14	range: 7–15
AaA		
Number	1.73 ± 1.01	3.27 ± 1.27
	range: 0–4	range: 1–5
Ø [µm]	25.71 ± 6.22	25.19 ± 9.50
	range: 17.02–40.02	range: 17.93–79.49
Between DA branches	0	21
Between adjacent DAs	9	54
AU		
Ø [µm]	25.87 ± 6.46	25.19 ± 9.50
	range: 17.02–40.02	range: 17.93–79.49
Area [mm^2]	1.62 ± 1.34	1.80 ± 1.56
Overlapping area [mm^2]	0.90 ± 0.91	0.68 ± 0.83

AaA, arterio-arterial anastomosis; AU, arterial unit; DA, dermal artery; HA, arteries in the hypodermal/dermal junction; LA, lateral artery.

an area of 1.80 ± 1.56 mm^2. Branches of neighbouring dermal arteries overlapped in a total area of 0.68 ± 0.83 mm^2 (Fig. 2D).

Discussion

Detailed knowledge of the architecture of arteries supplying blood to the epidermis and dermis is essential for understanding the genesis of skin pathologies, for researching the mechanisms underlying wound healing and for designing skin flaps. Anatomical and dermatological textbooks (Braverman, 2000; Kanitakis, 2002; Fritsch, 2009) describe two arterial plexi in thick and thin skin: a profound arterial plexus at the dermo/hypodermal junction and a

superficial arterial plexus in the papillary dermis. Recently, it was demonstrated that a superficial dermal arterial plexus does not exist in the thick skin of the thumb pad (Geyer et al. 2013). Instead, discrete arteries enter the dermis, ascend and ramify in a tree-like fashion and form terminal branches that reach a circumscript area of the superficial dermis. The dermal volume supplied by a single dermal artery was termed an 'arterial dermal unit'. The average superficial epidermal area overlying such a unit was approximately 1.70 ± 1.44 mm^2. The branches of the dermal arteries were connected through a mean of 2.50 ± 1.37 arterio-arterial anastomoses.

Our results, based on 3D analysis of 22 skin biopsies harvested from thin skin of the distal medial femur, show that the arterial supply to the superficial dermis of the cutaneous angiosome of the DGA is also organised in dermal arterial units. The epidermal area of these units is more variable than in the thumb pad (0.31–5.29 mm^2) and is on average slightly bigger (0.77–1.88 mm^2). The branches of the dermal arteries are connected by a similar number of arterio-arterial anastomoses (2.27 in thick skin of the thumb vs. 2.50 in the vascular territory of the DGA).

The central intention of this study was to test whether dermal arteries are organised in dermal arterial units in thin skin and whether this is true for the centre and the periphery of cutaneous angiosomes. For three reasons, we chose to study this by examining the architecture of the dermal arteries in the cutaneous vascular territory of the DGA. First, the DGA is easy to dissect due to its relatively constant course and its anatomical relation to the vasto-adductor membrane. Secondly, it is a relatively large artery, which can be easily cannulated or perfused via the femoral artery. Thirdly, its neighbouring cutaneous vascular territories can be simultaneously perfused via the popliteal artery. In a strict sense, our findings regarding the architecture of the dermal arteries of thin skin are therefore restricted to describing the situation in the cutaneous angiosome of the DGA. Yet, we consider it as likely that other areas covered with thin skin show a similar arrangement. However, further studies are required to prove this assumption.

Up to now, most studies analysing dermal arteries made use of corrosion casts and traditional histology (Yen & Braverman, 1976; Inoue, 1978; Braverman, 2000; Kanitakis, 2002). But traditional histological sections do not permit 3D visualisations and are therefore insufficient for analysing the complex architecture of dermal blood vessels. The corrosion cast technique, on the other hand, creates physical 3D models of blood vessels by filling the vessels with a permanent medium and eliminating the surrounding tissues. However, in the filling models, expert knowledge is required to distinguish between small arteries and small veins. To make this distinction, impressions caused by endothelial cell nuclei and scanning electron microscopy for their detection have been suggested (Sangiorgi et al. 2004). Additionally, they display different gross morphological
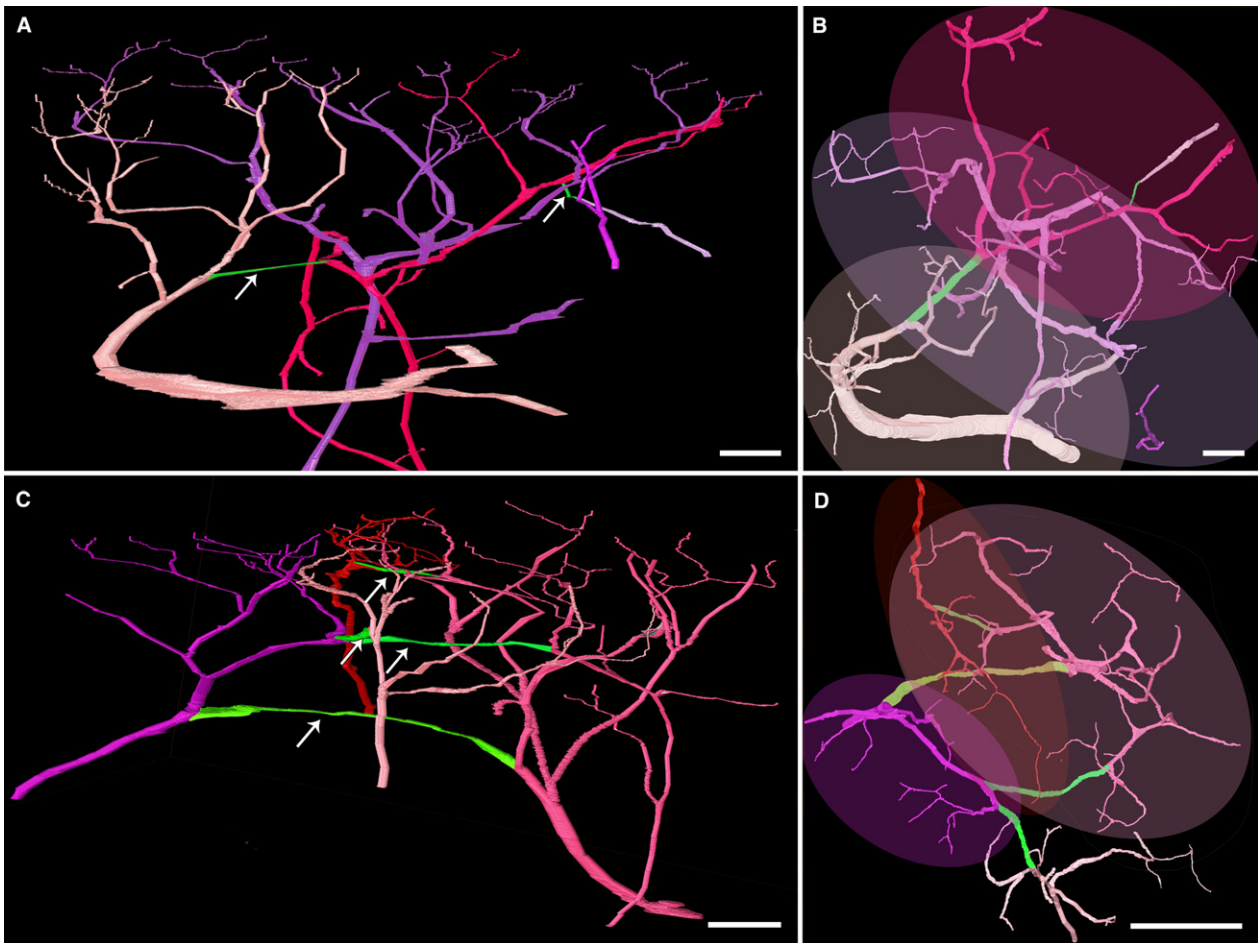
Fig. 2 Dermal vascular units. 3D surface models of the arteries (light pink, dark pink, purple and red) and arterio-arterial anastomoses (green, pointed with arrows) in the centre of the DGA angiosome (A,B) and the zone of overlap with the angiosomes of the popliteal artery (C,D). Again, the different colours of the arteries facilitate distinction and clearly highlight their interconnectedness. Lateral (A,C) and superficial views (B,D). The superficial views (B,D) show the extension of the vascular units as oval overlays. Note the extensive overlapping area of arterial units. Scale bars: 250 μm.

patterns reflecting their endo-luminal pressure properties. But although the distinction between arteries and veins is possible in corrosion casts, due to the complexity of models displaying both the arterial and the venous blood vessel network, the excess of information might be more of a hindrance than a help for analysing the interconnectedness of dermal arteries.

We therefore chose to employ the HREM technique for creating digital volume data from biopsy material harvested from skin areas representative for thin skin. From the data we created virtual 3D computer models of the dermal arteries and their branches by identifying large hypodermal arteries and following their branches through the entire data volume. This enabled us solely to visualise the dermal arteries, their branches and connections. No veins and no capillaries, except for exemplary capillaries arising from the terminal branches of the dermal arteries, were visualised or analysed. We consider this approach crucial to be able to distinguish between the branches of the dermal arteries

and the vessels feeding and forming the subpapillary venous plexus.

Neighbouring dermal arterial units are connected by arterio-arterial anastomoses. One of the hypotheses of our study was that the number of such anastomoses differs between the centre of the cutaneous angiosome of the DGA and the zone where it overlaps with neighbouring angiosomes. Our results verified this hypothesis. They revealed that at the level of the papillary dermis not a plexus but more arterio-arterial anastomoses secure the smooth blood exchange between neighbouring vascular territories.

Numerous studies show that there is significant blood exchange between cutaneous angiosomes (Taylor & Palmer, 1987; Saint-Cyr et al. 2009). As the arterial anastomoses within the dermis are small and their lumina are of relatively small diameters, our results suggest that this blood exchange is mainly secured by the profound arterial plexus and other subcutaneous anastomoses. However, due to the

relatively small size of the examined biopsies we were unable to analyse the architecture of the subcutaneous arteries and the profound arterial plexus to confirm this assumption.

One limitation of HREM is its *ex vivo* character. The tissues must be subjected to histological specimen processing involving dehydration in ethanol and immersion in resin. The fixation process was done beforehand without pressure perfusion due to technical limitations. Therefore, the processed biopsies experience tissue shrinkages of approximately 20%, and this may even vary slightly between specimens (Weninger et al. 2009). Moreover, the vessel calibers of the specimen could possibly suffer additional dimensional changes after perfusion with dyed Ringer solution. This has to be considered when interpreting measurements of the diameters of the arteries and their anastomoses.

Conclusions

We show that at least in the thin skin of the cutaneous vascular territory of the DGA the dermal arteries do not form a superficial dermal arterial plexus. Rather, they are organised in discrete dermal arterial units, which supply blood to circumscript volumes of the epidermis and superficial dermis. The branches of the dermal arteries are connected by a small number of arterio-arterial anastomoses. Their number is significantly smaller in the centre of the vascular territory of DGA compared with the overlapping zone with neighbouring cutaneous vascular territories. These results have important implications for interpreting, diagnosing and researching vascular pathologies and wound-healing processes.

Acknowledgements

Author contributions

Ines E. Tinhofer: acquisition of data, data analysis, statistical calculations, interpretation of data, drafting of the manuscript, creation of figures and tables. Maximilian Zaussinger: acquisition of data, data analysis, creation of figures. Stefan H. Geyer: acquisition of data, data analysis, statistical calculations, interpretation of data, drafting of the methods section of the manuscript, support in creating figures, critical revision of the manuscript. Stefan Meng: interpretation of data, critical revision of the manuscript. Lars-Peter Kamolz: contributions to study concept, critical revision of the manuscript. Chieh-Han J. Tzou: contributions to study concept and design, critical revision of the manuscript. Wolfgang J. Weninger: contributions to study concept and design, data analysis, interpretation of data, drafting of the discussion section of the manuscript, critical revision of the manuscript.

References

Braverman IM (2000) The cutaneous microcirculation. *J Investig Dermatol Symp Proc* **5**, 3–9.

Braverman IM, Keh A, Goldminz D (1990) Correlation of laser Doppler wave patterns with underlying microvascular anatomy. *J Invest Dermatol* **95**, 283–286.

Dalimier E, Salomon D (2012) Full-field optical coherence tomography: a new technology for 3D high-resolution skin imaging. *Dermatology* **224**, 84–92.

Fritsch P (2009) *Dermatologie und Venerologie für das Studium*. Berlin: Springer.

Geyer SH, Mohun TJ, Weninger WJ (2009) Visualizing vertebrate embryos with episcopic 3D imaging techniques. *ScientificWorldJournal* **9**, 1423–1437.

Geyer SH, Nohammer MM, Tinhofer IE, et al. (2013) The dermal arteries of the human thumb pad. *J Anat* **223**, 603–609.

Geyer SH, Nohammer MM, Matha M, et al. (2014) High-resolution episcopic microscopy (HREM): a tool for visualizing skin biopsies. *Microsc Microanal* **20**, 1356–1364.

Geyer SH, Tinhofer IE, Lumenta DB, et al. (2015) High-resolution episcopic microscopy (HREM): a useful technique for research in wound care. *Ann Anat* **197**, 3–10.

Geyer SH, Maurer-Gesek B, Reissig LF, et al. (2017) High-resolution episcopic microscopy (HREM) – simple and robust protocols for processing and visualizing organic materials. *J Vis Exp* **125**, https://doi.org/10.3791/56071.

Hasegawa K, Pereira BP, Pho RW (2001) The microvasculature of the nail bed, nail matrix, and nail fold of a normal human fingertip. *J Hand Surg Am* **26**, 283–290.

Horstmann E (1957) *Die Haut. Haut und Sinnesorgane.* (ed. M€ollendorff Wv), pp. 198–207, Berlin: Springer.

Ikeda A, Umeda N, Tsuda K, et al. (1991) Scanning electron microscopy of the capillary loops in the dermal papillae of the hand in primates, including man. *J Electron Microsc Tech* **19**, 419–428.

Inoue H (1978) Three-dimensional observations of microvasculature of human finger skin. *Hand* **10**, 144–149.

Kanitakis J (2002) Anatomy, histology and immunohistochemistry of normal human skin. *Eur J Dermatol* **12**, 390–399; quiz 400-401.

Koshima I, Soeda S (1989) Inferior epigastric artery skin flaps without rectus abdominis muscle. *Br J Plast Surg* **42**, 645–648.

Kroll SS, Rosenfield L (1988) Perforator-based flaps for low posterior midline defects. *Plast Reconstr Surg* **81**, 561–566.

Manchot C (1983) *The Cutaneous Arteries of the Human Body*. New York: Springer.

Mohun T, Weninger WJ (2010) Episcopic three-dimensional imaging of embryos. In: *Imaging in Developmental Biology: A Laboratory Manual*. (ed. Sharpe J, Wong R), pp. 765–776, New York: Cold Spring Harbor Laboratory Press.

Mohun TJ, Weninger WJ (2012a) Embedding embryos for high-resolution episcopic microscopy (HREM). *Cold Spring Harb Protoc* **2012**, 678–680.

Mohun TJ, Weninger WJ (2012b) Episcopic three-dimensional imaging of embryos. *Cold Spring Harb Protoc* **2012**, 641–646.

Mohun TJ, Weninger WJ (2012c) Generation of volume data by episcopic three-dimensional imaging of embryos. *Cold Spring Harb Protoc* **2012**, 681–682.

Saint-Cyr M, Wong C, Schaverien M, et al. (2009) The perforasome theory: vascular anatomy and clinical implications. *Plast Reconstr Surg* **124**, 1529–1544.

Sangiorgi S, Manelli A, Congiu T, et al. (2004) Microvascularization of the human digit as studied by corrosion casting. *J Anat* **204**, 123–131.

Spalteholz W (1927) *Blutgefäße der Haut. Anatomie der Haut*. Berlin: Springer.

Taylor GI, Minabe T (1992) The angiosomes of the mammals and other vertebrates. *Plast Reconstr Surg* **89**, 181–215.

Taylor GI, Palmer JH (1987) The vascular territories (angiosomes) of the body: experimental study and clinical applications. *Br J Plast Surg* **40**, 113–141.

Weninger WJ, Geyer SH, Mohun TJ, et al. (2006) High-resolution episcopic microscopy: a rapid technique for high detailed 3D analysis of gene activity in the context of tissue architecture and morphology. *Anat Embryol (Berl)*, **211**, 213–221.

Weninger WJ, Maurer B, Zendron B, et al. (2009) Measurements of the diameters of the great arteries and semi-lunar valves of chick and mouse embryos. *J Microsc* **234**, 173–190.

Wiedner M, Tinhofer IE, Kamolz LP, et al. (2014) Simultaneous dermal matrix and autologous split-thickness skin graft transplantation in a porcine wound model: a three-dimensional histological analysis of revascularization. *Wound Repair Regen*, **22**, 749–754.

Wong R, Geyer S, Weninger W, et al. (2016) The dynamic anatomy and patterning of skin. *Exp Dermatol* **25**, 92–98.

Yen A, Braverman IM (1976) Ultrastructure of the human dermal microcirculation: the horizontal plexus of the papillary dermis. *J Invest Dermatol* **66**, 131–142.

Zhang EZ, Povazay B, Laufer J, et al. (2011) Multimodal photoacoustic and optical coherence tomography scanner using an all optical detection scheme for 3D morphological skin imaging. *Biomed Opt Express* **2**, 2202–2215.